Analytical Biochemistry 380 (2008) 91–98

Contents lists available at ScienceDirect

Analytical Biochemistry

journal homepage: www.elsevier.com/locate/yabio

Green fluorescent protein (GFP) as a direct biosensor for mutation detection: Elimination of false-negative errors in target gene expression

Yu Kyung Tak [a], Pravin K. Naoghare [a], Kyeong-Hee Lee [b], Soon-Sup Park [c], Joon Myong Song [a,*]

[a] Research Institute of Pharmaceutical Sciences and College of Pharmacy, Seoul National University, San 56-1, Gwanak-gu, Seoul-151-742, Republic of Korea
[b] Applied Imaging Research Group, Korea Electrotechnology Research Institute, Gyeonggi-Technopark 1271-11, Ansan 426-901, Republic of Korea
[c] NANO Bio Research Center, Korea Electronics Technology Institute (KETI) #68, Yatop-Dong, Bundang-Gu, Sungnam-Si, KyungKi-Do 463-816, Republic of Korea

ARTICLE INFO

Article history:
Received 28 March 2008
Available online 24 May 2008

Keywords:
Green fluorescent protein
Direct biosensor
Mutagenic efficacy

ABSTRACT

A new method was developed to determine the mutagenic efficacy of a suspected mutagen by employing green fluorescent protein (GFP) as a direct biosensor for mutation detection. Alterations in target gene (AcGFP1) expression after mutagen [(±)-7*p*,8*a*-dihydroxy-9*a*,10*a*-epoxy-7,8,9,10-tetrahydrobenzo[*a*]pyrene (BPDE)] treatment were measured to detect the mutagenic efficacy of the carcinogen. In contrast to mutagen treatment of the entire plasmid or cell culture, the target AcGFP1gene devoid of the plasmid backbone was exposed to BPDE (10–500 μM) to eliminate the need for an additional fusion gene. Shuttle vectors (pAcGFP-N1) were religated to the AcGFP1 gene with BPDE adducts (0–8.59 μM) and replicated in the eukaryotic host. This approach eliminated false-negative errors in target gene expression that arose from BPDE adduct formation in the residual plasmid backbone rather than in the AcGFP1 gene. Determination of the BPDE–AcGFP1 adducts allowed the quantitative mutagenic effect of the BPDE adducts on AcGFP1 gene expression to be monitored. The results obtained with flow cytometry and confocal microscopy validate our method and demonstrate efficient and direct use of GFP as a biosensor for mutation detection.

Various biosensors have been developed to investigate the mutagenic potential of carcinogens based on either altered nucleotide sequence or protein expression. Methods based on an altered DNA profile [1,2] are limited when determining the active sites of the mutated gene sequence and its impact on altered protein expression, especially when adduct-forming mutagens are examined. In this context, the study available reported [3] that mutation hotspots do not correlate with hotspots of damage. To discern the fidelity of target gene expression while determining the mutagenic potential of carcinogens, several complicated vector constructs (GFP[1] reporter systems) with fusion genes have been used. Recently, specially constructed fusion vector systems [4,5] in combination with an appropriate reporter gene like sup F [6] have been used to detect mutations in mammalian cells, both in vivo and in vitro. However, these systems require several days or weeks to enumerate and characterize the mutants. The other important aspect of predicting the mutagenic efficacy of carcinogens on target genes is the mutagen treatment strategy. When the entire plasmid [7] or entire cell culture [8,9] is treated with mutagen, the mutagen may form adducts with the reporter gene, the plasmid backbone, or other cellular entities, as well as with the target gene, leading to erroneous results. When such strategies are used, mutagen treatment of GFP fusion vectors [9,10] may result in adverse mutagenic effects on the GFP reporter, as mutations in GFP reportedly alter its fluorescence [11,12]. Thus, visualization of altered gene expression in mammalian cells is highly desirable.

To eliminate the need for complicated vector constructs, we developed a method in which the native fluorescence of mutagen-treated GFP is monitored at the mammalian single-cell level without a fusion gene insert to detect mutations. GFP is one of the most common reporter domains used to detect mutations [13] as it does not require any substrates or cofactors [14]. Moreover, GFP is nontoxic to mammalian cells and its measurement is simple and reagent-free. Rather than treating the entire plasmid, we treated a restriction endonuclease-digested AcGFP1 fragment from the pAcGFP1-N1 vector with (±)-*trans*-7,8-dihydroxy-anti-9,10-epoxy-7,8,9,10-tetrahydrobenzo[*a*]pyrene (BPDE), a highly reactive electrophilic metabolite of benzo[*a*]pyrene reported to cause cytotoxicity and point mutations [15] in both prokaryotic and eukaryotic cells [16]. Elimination of false-negative errors in target gene expression, along with early adduct determination, adds an extra dimension and increases accuracy in determining the mutagenic concentrations responsible for altered expression of a targeted biomolecule. The data presented here demonstrate excellent utilization of GFP as a direct biosensor for mutation

* Corresponding author. Fax: +82 2 871 2238.
E-mail address: jmsong@snu.ac.kr (J.M. Song).

[1] *Abbreviations used:* GFP, green fluorescent protein; BPDE, (±)-*trans*-7,8-dihydroxy-anti-9,10-epoxy-7,8,9,10-tetrahydrobenzo[*a*]pyrene; THF, tetrahydrofuran.

0003-2697/$ - see front matter © 2008 Elsevier Inc. All rights reserved.
doi:10.1016/j.ab.2008.05.029

detection and a new method to fortify biosensor technology. Analyzing GFP expression through flow cytometry is an excellent choice for detection at the level of single mammalian cells.

Materials and methods

Cells and plasmids

Human embryonic kidney cells (HEK 293) were cultured in Dulbecco's modified Eagle's medium. Cultures were supplemented with 10% (v/v) fetal bovine serum (16000-044, Gibco), 60 μg/ml penicillin, and 100 μg/ml streptomycin (P0781, Sigma) and maintained in 25-cm^2 cell culture flasks (Nunclon) at 37 °C under 5% CO_2. A 4700-bp shuttle vector, pAcGFP1-N1, encoding GFP was obtained from Clontech (Palo Alto, CA, USA) (Fig. 1).

Transformation and amplification of target genes

Competent *Escherichia coli* DH5α cells were subjected to chemical transformation as suggested by the manufacturer (Invitrogen, Carlsbad, CA, USA). The transformants were selected on Luria broth agar plates supplemented with kanamycin (30 μg/ml). Plasmids from resistant colonies were isolated using a Plasmid Midi Kit (Qiagen, Valencia, CA, USA). AcGFP1 fragments were then subjected to restriction endonuclease digestion (EcoRI/NotI) amplification with specific primers, AcGFP1 (5′-GCTTCGAATTCTGCAGTCGACGG) and AcGFP2 (5′-AGTCGCGGCCGCTCACTTGTACA), according to the following temperature profile: 94 °C for 5 min, 30 cycles of 94 °C for 30 s, 55 °C for 30 s, 72 °C for 30 s, and a final extension at 72 °C for 5 min. PCR amplification was confirmed by analyzing the amplified 766-bp AcGFP1 fragment on 1% agarose gel with standard molecular weight markers.

BPDE adducts on AcGFP1 gene fragment

Before BPDE treatment, the amplified AcGFP1 DNA was dissolved in 5 mM sodium cacodylate buffer solution supplemented with 0.1 M NaCl and 3 mM EDTA. Metal ions and other impurities were removed by dialysis against 5 mM sodium cacodylate buffer to prevent possible interference [17] with the fluorescence properties of GFP. Aliquots of solid racemic BPDE (NCI Chemical Carcinogen Repository, Midwest Research Institute, Kansas City, MO, USA) were prepared in a small volume of anhydrous tetrahydrofuran (THF). BPDE adducts on the AcGFP1 gene fragment were designated *G1*. DNA (AcGFP1) solutions (5×10^{-7} M) were incubated at room temperature in the dark with various BPDE concentrations at specific time intervals—1×10^{-5} M (12 h), 1×10^{-5} M (48 h), 1×10^{-4} M (24 h), and 5×10^{-4} M BPDE (48 h)—to yield the first, second, third, and fourth BPDE–AcGFP1, adducts, respectively (Fig. 2a). The final THF concentration in all reaction mixtures was below 1%. Repeated ether extractions, followed by ethyl alcohol precipitation, were performed to remove the tetrasol produced by the hydrolysis of BPDE. Finally, the DNA was dissolved in 5 mM sodium cacodylate buffer solution For early adduct determination, the number of moles of BPDE bound per mole of DNA was determined by absorption at 346 nm (extinction coefficient = 29,000 M^{-1} cm^{-1}) within the total spectral range 300–370 nm. BPDE–AcGFP1 adducts (G1) were confirmed by UV spectroscopy and, along with the untreated AcGFP1, were ligated as suggested by the manufacturer (Clontech). DNA samples treated under identical conditions but without BPDE were used as the control. The BPDE-treated AcGFP1 DNA and the pAcGFP-N1 vector with BPDE–AcGFP1 adducts were analyzed for altered mobility shift on 1% agarose gel (Fig. 2b).

Transfections

The recircularized plasmids (G1) were transfected (in triplicate) into HEK 293 cells under the appropriate culture conditions. On the following day, the cells were transfected using Lipofectamine 2000 (Invitrogen) according to the manufacturer's instructions.

DNA sequencing and multiple sequence alignment

DNA sequence analysis of the AcGFP1 gene (with BPDE adducts) was performed 48 h after transfection (Fig. 3a). Plasmids were prepared using a slight modification of the standard QIAprep Spin Miniprep method. Plasmid sequencing was carried out using AcGFP1 (5′-GCTTCGAATTCTGCAGTCGACGG) and AcGFP2 (5′-

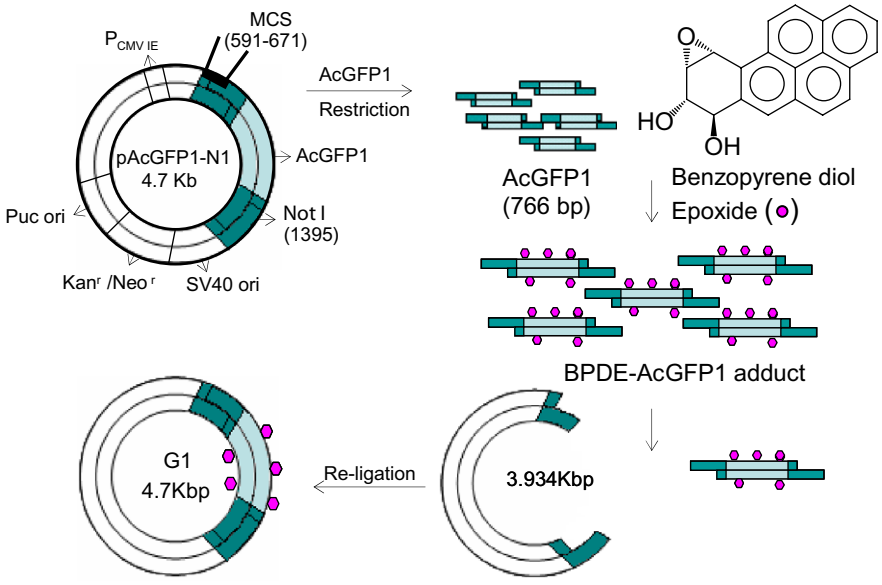

Fig. 1. Schematic representation of pAcGFP1-N1 shuttle vector and mutagen treatment strategy. AcGFP1 gene (766 bp) was restriction digested from the shuttle vector and then treated with BPDE. Different concentrations of BPDE–AcGFP1 adducts were religated into the pAcGFP1-N1 vector, as was the control (BPDE–untreated AcGFP1). These constructs were then transfected into HEK 293 cells.

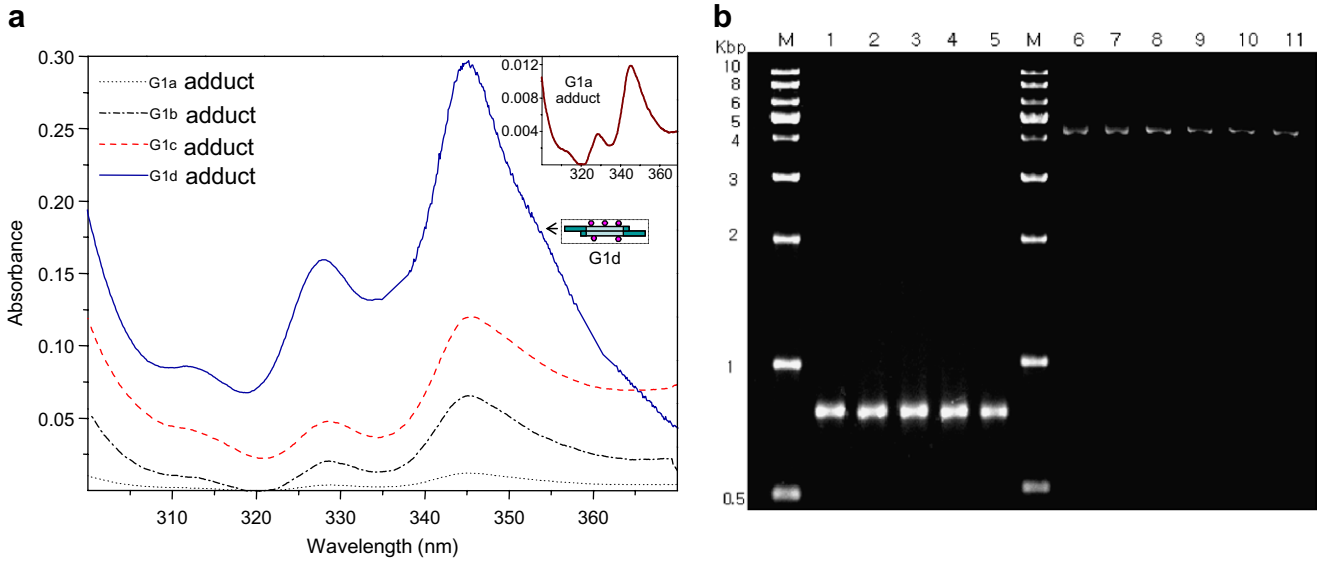

Fig. 2. Formation of BPDE–AcGFP1 adducts after BPDE treatment. (a) UV spectra illustrate a linear increase in absorbance (spectral range 300–370 nm) with increasing concentration of BPDE–AcGFP1 adducts at different time intervals (absorption maximum = 346 nm). Inset: spectrum representing the lowest (G1a) BPDE–DNA adduct concentration on a smaller absorbance scale. (b) Gel image (1% agarose) of the 766-bp AcGFP1 DNA (lanes 1–5) and the religated pAcGFP1-N1 vector (lanes 6–11). Lane 1 represents AcGFP1 DNA (BPDE untreated) and lanes 2–5 represent the first, second, third, and fourth BPDE–AcGFP1 adducts. Similarly, lanes 6 and 7 represent untreated pAcGFP1-N1 vector. Lanes 8–11 represent the pAcGFP1-N1 vector religated with G1a, G1b, G1c, and G1d adducts.

AGTCGCGGCCGCTCACTTGTACA) primers and 500 ng plasmid DNA. The resulting sequences were analyzed with MultAlin multiple sequence alignment software (Fig. 3b).

Confocal microscopy and flow cytometry of fluorescent cells

Flow cytometric analysis (Fig. 4a) and confocal microscopy (Fig. 4a, inset) of HEK 293 cells (in triplicate) were performed 48 h after transfection. Confocal micrographs were obtained with an inverted confocal microscope (Olympus Model IX71) and analyzed with Meta Imaging Series 6.3 software (Molecular Devices, Downingtown, PA, USA). Alterations in GFP fluorescence measured via flow cytometric analysis (Fig. 4b1) and confocal microscopy (Fig. 4b2) were plotted as a function of BPDE–AcGFP1 adduct concentrations.

BPDE adduct on pAcGFP1-N1 plasmid backbone devoid of AcGFP1 gene

BPDE adducts on plasmid backbone (3934 bp) devoid of AcGFP1 gene fragment were designated *P1*. Adducts (adducts 1, 2, 3, and 4) were ligated to non-BPDE-treated AcGFP1 genes. Except for the DNA (P1 instead of G1), all other experimental conditions for ligation and transfection were similar to those described above. Alterations in GFP fluorescence observed by flow cytometric analysis were plotted as a function of BPDE-plasmid backbone adduct concentration (Fig. 5).

BPDE adduct on whole plasmid

BPDE adducts on whole plasmids with AcGFP1 gene fragments were designated *PG1*. Plasmid (pAcGFP1-N1) solutions (1.45 μg/μl in 150 μl) were incubated at room temperature in the dark with various concentrations of BPDE at specific time intervals: 1×10^{-5} M (12 h), 1×10^{-5} M (48 h), 1×10^{-4} M (24 h) and 5×10^{-4} M (48 h) BPDE. Other experimental conditions were similar to those mentioned above. Plasmids were further digested with EcoRI–NotI restriction enzymes to yield the 3934-bp plasmid backbone and the 766-bp AcGFP1 gene fragment. Plots of absorption spectra of BPDE–DNA adducts formed on the 3934-bp plasmid backbone against increasing BPDE concentration/time are labeled adduct 1, adduct 2, adduct 3, and adduct 4, whereas plots of adducts formed on the 766-bp AcGFP1 gene are labeled adduct 1a, adduct 2a, adduct 3a, and adduct 4a (Fig. 6a). The number of moles of BPDE residues bound per mole of DNA was determined from the absorption at 346 nm, as described above. The concentrations of BPDE adducts formed on the 766-bp AcGFP1 gene were compared from the absorption spectra following treatment of the entire plasmid or only the AcGFP1 gene with BPDE (Fig. 6b).

Results

BPDE–AcGFP1 adducts in the pAcGFP1-N1 vector

The pAcGFP1-N1 shuttle vector (Fig. 1) encoding the AcGFP1 gene was used to monitor the mutagenic potency of BPDE. In this approach, the AcGFP1 gene was intentionally restriction digested from the shuttle vector to yield different concentrations of BPDE–AcGFP1 adducts (G1). As shown in Fig. 1, BPDE–AcGFP1 adducts were then religated into the shuttle vector (pAcGFP1-N1).

Characterization of the BPDE-treated AcGFP1 gene

BPDE-treated AcGFP1 DNA was assayed to determine the moles of BPDE residues bound per mole of DNA. Over the range 300–370 nm (Fig. 2a), the absorption spectra of BPDE-treated DNA displayed a linear relationship with respect to BPDE concentration and incubation time. The molar BPDE–adduct concentrations calculated were 4×10^{-7}, 2.24×10^{-6}, 4.1×10^{-6}, and 8.59×10^{-6} M and designated as G1a, G1b, G1c, and G1d BPDE–AcGFP1 adducts, respectively. BPDE–AcGFP1 adducts displayed an intact band at the same position (766 bp) as the control (BPDE–untreated). The religated pAcGFP-N1 vector containing the BPDE–AcGFP1 adducts also generated the desired 4.7-kb band on 1% agarose gel (Fig. 2b), similar to the commercially available pAcGFP-N1 vector.

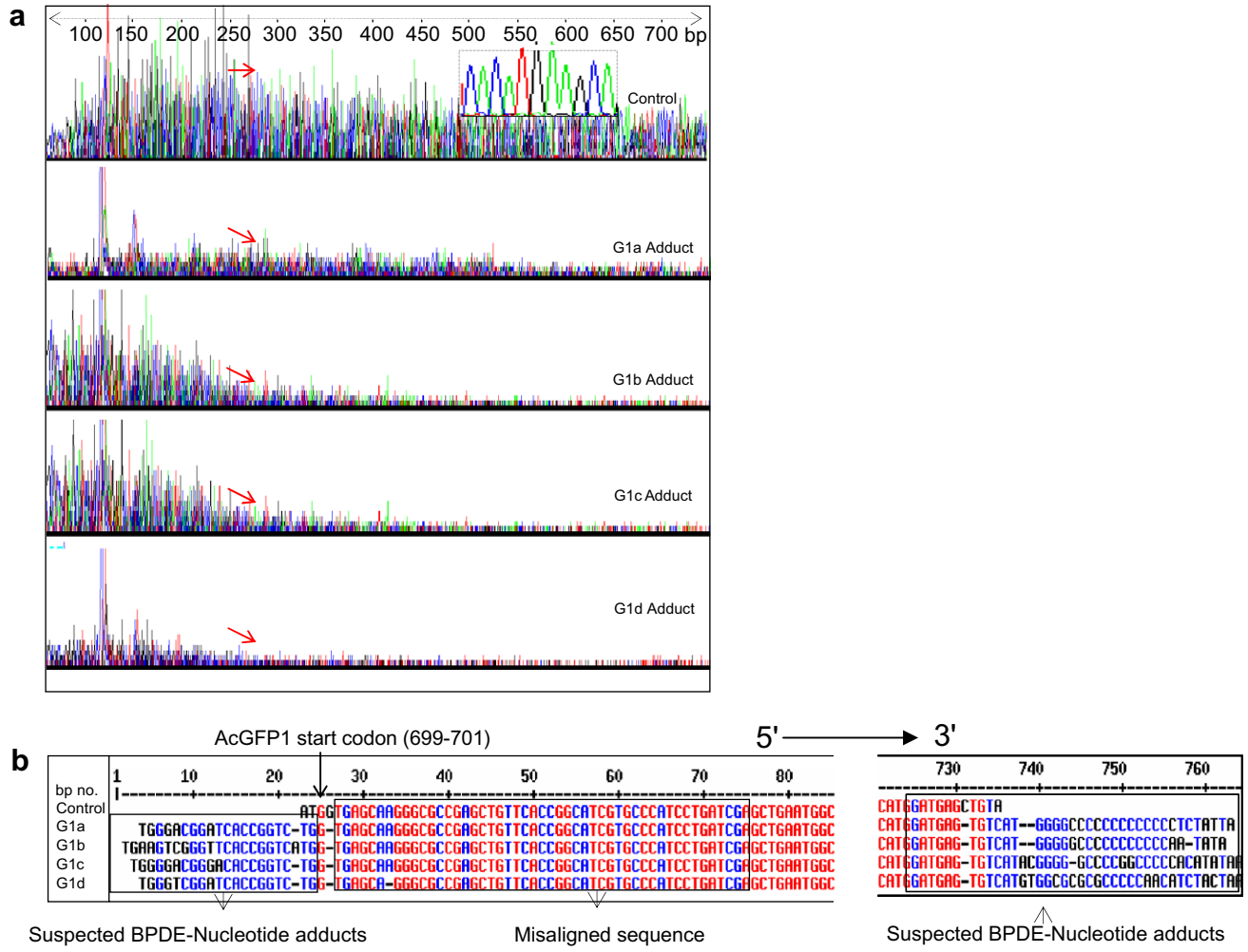

Fig. 3. (a) DNA sequencing of AcGFP1 gene (with BPDE adducts) 48 h after transfection. The chromatogram depicts the effect of BPDE–AcGFP1 adducts on the nucleotide sequence of the AcGFP1 gene. Inset: enlarged chromatogram of the control sample. Compared with the control, nucleotide signal intensity gradually decreased (red arrow) when BPDE adduct-containing DNA was sequenced. (b) Multiple sequence alignment with hierarchical clustering of BPDE-treated DNA with control. Heterogeneity in nucleotide sequences can be observed at both the 5′ and 3′ ends. This may be a consequence of BPDE–nucleotide adduct formation in the cycle sequencing PCR. (For interpretation of the references in colour in this figure legend, the reader is referred to the web version of this article.)

Effect of BPDE–AcGFP1 adducts (G1) on DNA sequencing

The control (not treated with BPDE) exhibited high nucleotide signal intensity throughout the chromatogram with minimum signal-to-noise ratio (Fig. 3). This illustrates that almost equal copy numbers of each DNA fragment were formed during the cycle sequencing PCR. In contrast, a gradual decrease (red arrow) in nucleotide signal intensity (after ~250 bp) was observed in BPDE-treated samples (Fig. 3a). Indeed, nucleotide signal intensity was inversely proportional to BPDE–AcGFP1 adduct concentration. Multiple sequence alignment with hierarchical clustering of BPDE-treated DNA with control revealed interesting results. Initial nucleotide sequences at both the 5′ and 3′ ends were heterogeneous (suspected BPDE–nucleotide adducts), and the sequences were misaligned up to 75 bp. This may be due to BPDE adduct formation on residual dideoxynucleotides in the cycle sequencing PCR. Later sequences (after 75 bp) were in better homology. This indicates that BPDE–DNA adduct formation interfered considerably with the polymerization DNA template in cycle sequencing PCR, resulting in the formation of low-molecular-weight fragments with misincorporated nucleotide bases. The later (after 80 bp) homologous DNA strands appeared to be in low copy number in the chromatogram. This may be the outcome of sequencing using a template DNA (plasmid) without BPDE–DNA adducts (even after BPDE treatment). Considering the ineffectiveness of DNA sequencing in determining mutations (especially in adduct-forming mutagens), expression analysis was carried out via flow cytometry and confocal microscopy.

Localization and quantitation of subcellular fluorescent protein

The progenies of the BPDE–AcGFP1 adduct (G1)- and BPDE–plasmid backbone (3934 bp) adduct (P1)-containing plasmids were monitored by flow cytometric analysis to determine the mutagenic potency of BPDE in the expression of GFP. Four different BPDE–AcGFP1 adducts were religated into the pAcGFP1-N1 plasmid backbone (without BPDE treatment) and transfected into the eukaryotic host (HEK 293 cells). Similarly, BPDE–plasmid backbone adducts were religated with the untreated AcGFP1 fragment and transfected into HEK 293 cells. Considering the doubling time (~10 h) of HEK cells, GFP expression was monitored by flow cytometry 48 h after transfection to allow more than four cycles of plasmid replication in the eukaryotic environment. Fig. 4a comprises the histograms for the control and four different BPDE–AcGFP1 adducts obtained by flow cytometry. The molar BPDE concentrations of BPDE–AcGFP1 adducts G1a, G1b, G1c,

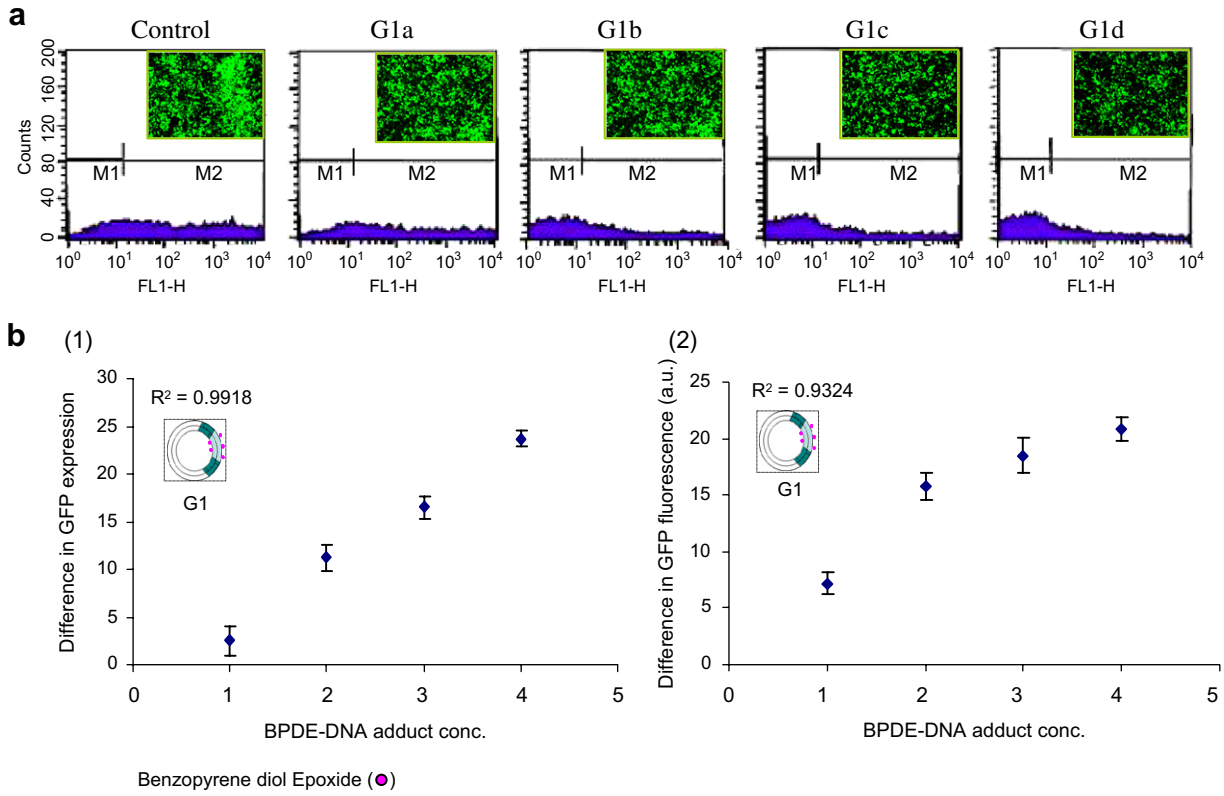

Fig. 4. Non-BPDE-treated plasmids or plasmids containing BPDE–AcGFP1 adducts, 48 h after transfection in HEK 293 cells. (a) Histogram illustrating the linear decrease in GPF expression (M2 region) with increasing concentration of BPDE–AcGFP1 adducts (i.e., G1a, G1b, G1c, and G1d) compared with the non-BPDE-treated control. Inset: Confocal micrographs illustrate similar results, with GFP fluorescence decreasing as BPDE–AcGFP1 adduct concentration increases. (b1) Scatter graph illustrating the quantitative effect of BPDE–AcGFP1 adducts on percentage GFP expression. Values 1, 2, 3, and 4 on the *X* axis represent BPDE–AcGFP1 adduct concentrations from 0.40 to 8.59×10^{-6} M. The *Y* axis corresponds to the difference in percentage GFP expression between BPDE-treated cells and control. The error bars indicate the variations in GFP expression obtained from three transfection replicates of non-BPDE-treated plasmid (pAcGFP1-N1) and plasmids containing different concentrations of BPDE–AcGFP1 adducts in HEK cells. (b2) The *Y* axis corresponds to the difference in GFP fluorescence between BPDE-treated cells and control. With increasing concentration of BPDE–AcGFP1 adducts ($0.40–8.59 \times 10^{-6}$ M), the average signal intensity of GFP fluorescent cells decreases linearly (i.e., increase in the difference in GFP fluorescence) compared with the non-BPDE-treated control. The SDs indicate the variations in average signal intensity obtained from three transfection replicates of non-BPDE-treated plasmids and plasmids containing different concentrations of BPDE–AcGFP1 adducts in HEK cells.

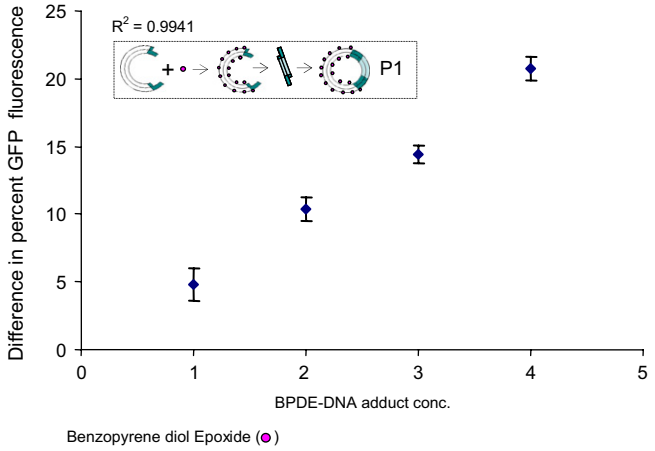

Fig. 5. Difference (compared with control) in percentage GFP fluorescence obtained by flow cytometric analysis of four different BPDE–plasmid backbone adducts, religated with AcGFP1 fragments (without BPDE treatment). See inset for details. The difference in percentage GFP fluorescence increased linearly with increasing concentrations of BPDE–plasmid backbone adducts. Error bars refer to the variations in GFP fluorescence obtained from three replicates.

and G1d were 4.00×10^{-7}, 2.24×10^{-6}, 4.10×10^{-6}, and 8.59×10^{-6} M, respectively. The inset (micrograph) represents the alteration in GFP expression at the corresponding BPDE concentration. Data clearly revealed a reduction in GFP expression (M2 region) with increasing concentration of BPDE adducts. More statistical information was obtained from a scatter graph. As shown in Fig. 4b1, the differences (compared with control) in the percentage GFP expression according to quantitative flow cytometric analysis were 2.47, 11.19, 16.49, and 23.71 for the G1a, G1b, G1c, and G1d BPDE-AcGFP1 adduct concentrations, respectively. The linear regression coefficient (R^2) was 0.9918. In Fig. 4a (inset) are confocal micrographs taken in fluorescence mode. To obtain better insight, average fluorescence intensity of the confocal micrographs was plotted against BPDE–AcGFP1 adduct concentration (Fig. 4b2). The average signal intensities of the confocal micrographs were 40.83, 33.62, 25, 22.33, and 20 for the control, G1a, G1b, G1c, and G1d BPDE–AcGFP1 adducts, respectively. The linear regression coefficient (R^2) was 0.9324. These results clearly demonstrated a substantial effect of BPDE on GPF expression. Fig. 5 displays the differences (versus control) in percentage GFP expression, as measured by flow cytometric analysis, of four P1 adducts. Differences in percentage GFP fluorescence were plotted against BPDE–plasmid backbone adduct (P1) concentration, that is, 3.55×10^{-5}, 1.00×10^{-6}, 1.58×10^{-6}, and 3.11×10^{-6} M (represented as 1, 2, 3, and 4 on the *X* axis, respectively). The differences in percentage GFP expression were 4.77, 10.34, 14.44, and 20.74 for the first, second, third, and fourth BPDE–plasmid backbone adduct (P1) concentrations, respectively. The linear regression coefficient (R^2) was 0.9941. Thus, increasing concentrations of BPDE–plasmid

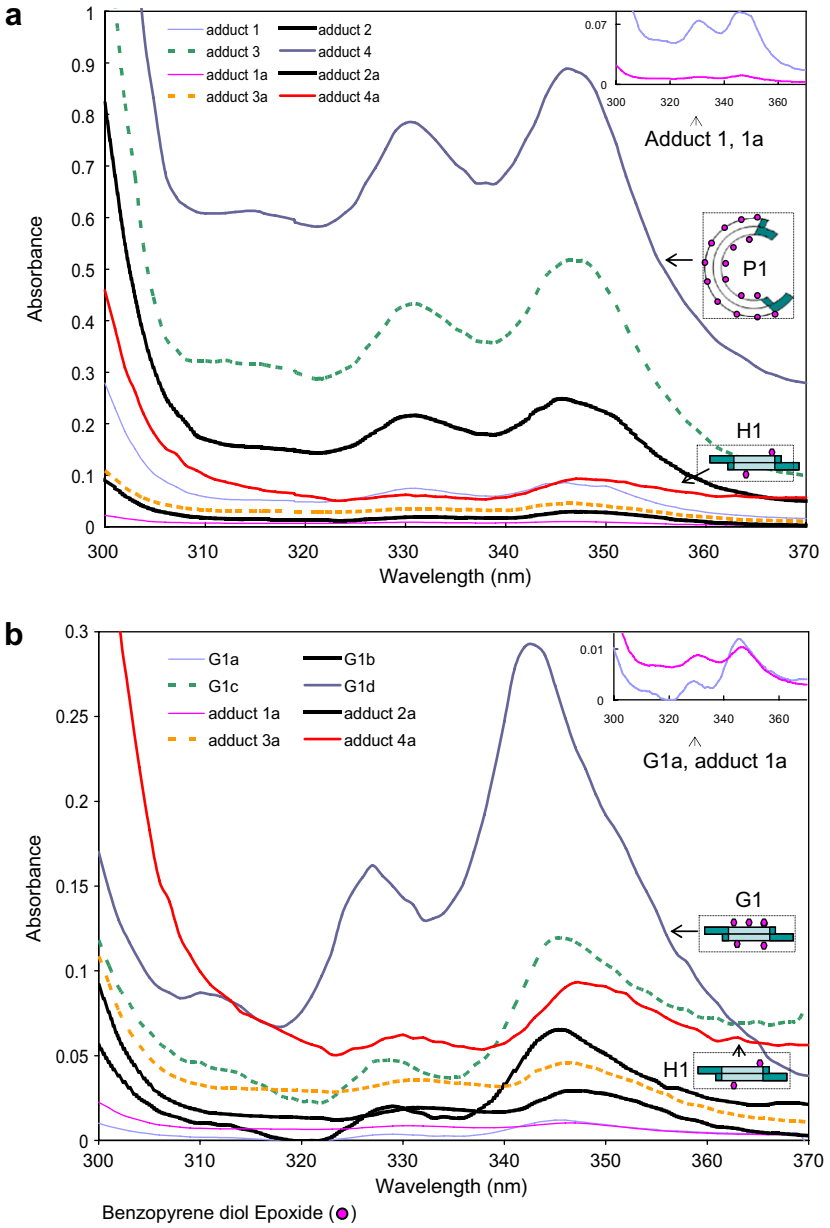

Fig. 6. (a) Entire plasmid was treated with BPDE at various concentrations and time intervals. Plasmids were restriction digested to yield the 3934-bp BPDE–plasmid backbone adducts (P1) 1, 2, 3, and 4 and the 766-bp BPDE–AcGFP1 adducts (H1) 1a, 2a, 3a, and 4a. UV spectra reveal a linear increase in absorbance over the spectral range 300–370 nm with increasing concentrations of BPDE–DNA adducts. Inset: Spectra representing the lowest BPDE–DNA adduct concentration (adduct 1 and 1a) on a smaller absorbance scale. (b) Equal copy numbers of adducts (H1) 1a, 2a, 3a, and 4a (in which AcGFP 1 gene restriction digestion followed treatment of the entire plasmid) abd G1a, G1b, G1c, and G1d (in which only the AcGFP1 gene was treated with BPDE) were compared over the spectral range 300–370 nm. Inset: spectra of G1a and adduct 1a. There were more BPDE–AcGFP1 adducts when only the AcGFP1 gene was exposed to BPDE compared to when the entire plasmid DNA was treated with BPDE.

backbone adducts resulted in proportional decreases in target gene (AcGFP1 gene) expression. This is clear evidence demonstrating the lacunas inherent in mutagen treatment of the whole plasmid. Hence it can be inferred that alterations in the plasmid backbone can considerably hamper target gene expression.

Mutagen treatment of target gene versus plasmid backbone

To fix the concentration of suspected mutagen with respect to a particular gene target, only the gene itself should be exposed to the mutagen and not the entire plasmid surrounding the target gene. To demonstrate this, equal numbers of copies of the AcGFP1 gene with and without plasmid backbone were used. Plasmid (4700 bp) concentration was 6.136 times higher than the concentration of target gene sequence, AcGFP1 (766 bp), considering the relative nucleotide lengths. Both demarcated forms (G1 and PG1) of DNA were exposed to various BPDE concentrations (see Materials and methods for details). PG1 was further restricted to yield P1 adducts 1, 2, 3, and 4 and H1 adducts 1a, 2a, 3a, and 4a (Fig. 6a). In the inset are the spectra of adducts 1 and 1a. Molar BPDE–DNA adduct concentrations were calculated as described and were 2.96×10^{-6}, 8.54×10^{-6}, 1.18×10^{-6}, 3.07×10^{-5}, 3.55×10^{-7}, 1.00×10^{-6}, 1.58×10^{-6}, and 3.11×10^{-6} M for adducts 1, 2, 3, 4, 1a, 2a, 3a, and 4a, respectively. Thus, adduct formation was proportional to BPDE concentration, and the majority of adducts formed on the plasmid backbone and not on the target gene. These results favor our proposed methodology and also call into question the strategy of treating the entire plasmid with mutagen. We also com-

pared adducts 1a, 2a, 3a, and 4a (AcGFP 1 gene restricted after treatment of entire plasmid treatment) with adducts G1a, G1b, G1c, and G1d (only AcGFP 1 gene treated with BPDE) (Fig. 6b). It should be noted that DNA copy numbers were similar. In the inset are the spectra of adducts G1a and 1a. Comparing the number of BPDE–AcGFP1 adducts formed on the target gene (AcGFP1) sequence with the number formed on the entire plasmid clearly demonstrated that more BPDE–DNA formed when only the target sequence, instead of the entire plasmid, was treated with BPDE. The probability of BPDE binding to the target gene decreased, as the plasmid backbone could also bind to BPDE.

Discussion

To develop selective measurement techniques, researchers are exploring biomolecules as direct sensors for diagnostics, toxicity assessment, and drug research. We have developed a method for determining the mutagenic efficacy of a suspected mutagen using GFP as a direct biosensor for mutation detection. Among the several approaches to detecting mutations, sensors based on altered DNA profiles are time consuming and cannot explain the effect on protein expression, especially when an adduct-forming mutagen (BPDE) is analyzed. Our results revealed misaligned sequences along with the suspected BPDE–nucleotide adducts at both the 5′ and 3′ ends of the AcGFP1 gene, in support of this hypothesis. These 5′ and 3′ modifications may cause truncated DNA fragments that terminate in the vicinity of the damaged site. However, the possibility of formation of BPDE adducts on residual dideoxynucleotides in the cycle sequencing PCR cannot be ruled out. In this context, a report illustrating the uneven distribution of BPDE-induced mutation hotspots (GC → TA transversions) suggests an ambiguity in base pair alterations with respect to gene expression. Indeed, the available literature suggests that BPDE interacts stereospecifically with prokaryotic and eukaryotic polymerases in vivo and that the conformational alterations caused by DNA polymerase–BPDE adduct interaction can alter the site of termination of DNA synthesis, which could be unique to individual polymerases [18]. Thus, mutations should be judged by actual alterations in nucleotide bases and not by the misincorporation of nucleotides by polymerases. The results obtained clearly indicate that treatment of the entire plasmid with mutagen may provide misleading data, as changes in target gene expression may result from dysfunction of the plasmid backbone and not from dysfunction of the target gene.

Because of the importance of expression analysis in mutation detection, several complicated vector constructs with fusion genes (e.g., GFP reporter systems) have been used as biosensors for mutation detection. GFP reporter systems have also been used as genotoxicity biosensors to screen genes involved in DNA repair [19]. However, reports elucidating the possible effects of mutagens on a target fusion genes based on GFP fusion vectors do not account for the adverse effect of the mutagen on GFP fluorescence. Even though GFP is stable in a variety of buffers and temperatures [10], there are reports that suggest a possible effect of mutations on GFP fluorescence [11,12]. Therefore, the possible effect of mutagens on GFP fluorescence, along with effects on the target fusion gene, may not be predictable. Moreover, mutagen treatment of the entire plasmid containing the target gene or of the entire cell culture can also damage residual plasmid DNA or other cellular entities, resulting in altered target gene expression, even without mutation. The plasmid backbone contains several important sequences that are directly or indirectly related to target gene expression. Moreover, the length of the plasmid backbone varies depending on the type of vector used in the experiment. Thus, the possibility of adduct formation to a targeted site (DNA) decreases when the entire plasmid, including the target gene, is treated as a whole. As a consequence, most adducts form on the plasmid backbone and, hence, the results may be misleading.

We developed an approach in which the target gene (AcGFP1) is exposed to BPDE to explore the possibilities of using GFP (without a fusion gene) as a direct biosensor for mutation detection. This approach eliminated the false-negative errors in target gene expression that arise from BPDE adduct formation in the residual plasmid backbone rather than in the AcGFP1 gene. Determination of the BPDE–AcGFP1 adduct through UV spectroscopy and validation of its effect on GFP expression in the eukaryotic environment practically obviated the need for further verification of the results obtained on altered gene expression.

New approaches for screening possible mutagens should be rapid, direct, and simple. However, systems that entail the enumeration and characterization of mutants are time consuming. Furthermore, these systems cannot determine whether mutations occur in the target gene or in the bacterial cells used to detect mutant genes [4]. In this study, confocal microscopy allowed visualization of subcellular GFP expression, whereas flow cytometric analysis provided quantitative GFP expression profiling. As shown in Fig. 4, GFP expression decreased linearly with increasing BPDE–AcGFP1 adduct concentration. This suggests a possible role for BPDE in altered GFP expression. BPDE adducts on various target genes have already been reported to cause point mutations [20–23], and we found that BPDE adducts interfere with GFP expression in HEK 293 cells. Thus, validation through confocal microscopy and flow cytometry supports this approach of employing GFP as a direct biosensor in determining the mutagenic potency of a mutagen.

In the approach developed here, the target gene (AcGFP1) was directly treated with a mutagen (BPDE) and then religated into the pAcGFP-N1 vector. However, this approach poses two interesting questions. First, apart from adduct formation, can BPDE also induce DNA cleavage? Second, does the BPDE–AcGFP1 adduct affect the efficiency of religation of AcGFP1 into the pAcGFP-N1 vector? DNA gel electrophoresis (Fig. 2b) revealed an intact band of BPDE–AcGFP1 adducts (766 bp) similar to the control on 1% agarose gel. This suggests that BPDE contributes only to adduct formation and not to DNA cleavage. Similarly, the religated pAcGFP-N1 vector containing the BPDE–AcGFP1 adducts was also the desired 4.7-kb size (Fig. 2b), identical to the commercially available pAcGFP-N1 vector. Thus, the vector was properly religated with the AcGFP1 target gene containing BPDE adducts, and adduct formation did not affect the efficiency of religation of the pAcGFP-N1 vector. Pommier and co-workers [24] have demonstrated that the inhibition of religation by carcinogenic adducts is predominantly responsible for the increase in top1 (DNA topoisomerase I)-mediated cleavage complexes, similar to top1 poisons like camptothecin [25–27]. BaPDE-2 (benzo[*a*]pyrene diol epoxide) adducts primarily enhanced the formation of topl cleavage complexes while exerting minimal effects on religation. As explained above, we did not observe cleavage of the AcGFP1 gene after BPDE adduct formation. This suggests that the effects of carcinogens on the cleavage complexes vary with the target DNA sequence. Thus, the minimal effect of BaPDE-2 adducts on religation reported by Pommier and co-workers [24] supports our findings.

The data obtained suggest that treatment of AcGFP1 with BPDE, followed by its religation into the pAcGFP-N1 vector and replication in human cells, subsequently reduces GFP expression and increases the concentration of BPDE adduct. Mukhopadhyay et al. [9] reported that the diffuse distribution of GFP in nuclear and cytoplasmic compartments of HEK 293 cells remained unchanged by BPDE treatment. However, the final concentrations of BPDE (0–0.2 μM) and the mutagen treatment strategy (entire culture) used in their study may explain this discrepancy. Mutagen treatment of the entire culture can result in reduced adduct formation on the target gene, as most of the BPDE molecules are engaged

with other cellular entities. In contrast, in the present study, the restricted AcGFP1 DNA was treated with higher BPDE concentrations (10–500 μM). Subsequently, BPDE–AcGFP1 adducts (0–8.59 μM), after religation and transfection, resulted in altered GFP expression in human cells.

Conclusion

We have described a method for the efficient use of GFP for mutation detection that eliminates false-negative errors. In contrast, the approach developed allows rapid early determination of BPDE adduct formation per mole of AcGFP1 DNA through UV spectroscopy before the religation step. In elucidating the mutagenic efficacy of a suspected mutagen, this approach allows selection of the initial concentration of adduct formed per mole of DNA. The data presented here demonstrate the employment of our method to strengthen biosensor technology by using GFP as a direct biosensor for mutation detection. This method nullifies false-negative errors and facilitates screening and determination of accurate mutagen concentration through early DNA–adduct determination.

Acknowledgments

This work was supported by a Korean Research Foundation grant funded by the Korean Government (MOEHRD, Basic Research Promotion Fund, KRF-2005-003-C00123) and by a Korea Science and Engineering Foundation (KOSEF) grant funded by the Korean government (MOST, M20704000042-07M0400-04210).

References

[1] N.M. Grubor, R. Shinar, R. Jankowiak, M.D. Porter, G.J. Small, Novel biosensor chip for simultaneous detection of DNA–carcinogen adducts with low-temperature fluorescence, Biosens. Bioelectron. 19 (2004) 547–556.
[2] C.A. Rowe-Taitt, J.P. Golden, M.J. Feldstein, J.J. Cras, K.E. Hoffman, F.S. Ligler, Array biosensor for detection of biohazards, Biosens. Bioelectron. 14 (2000) 785–794.
[3] V.M. Maher, J.L. Yang, M.C. Mah, J.J. McCormick, Comparing the frequency and spectra of mutations induced when an SV-40 based shuttle vector containing covalently bound residues of structurally-related carcinogens replicates in human cells, Adv. Exp. Med. Biol. 220 (1989) 83–92.
[4] M.J. Dycaico, G.S. Provost, P.L. Kretz, S.L. Ransom, J.C. Moores, J.M. Short, The use of shuttle vectors for mutation analysis in transgenic mice and rats, Mutat. Res. 307 (1994) 461–478.
[5] M. Jones, K. Burkhart-Schultz, A.V. Carrano, A method to quantify spontaneous and in vivo induced thioguanine-resistant mouse lymphocytes, Mutat. Res. 147 (1985) 97–105.
[6] C.A. Bigger, I. Ponten, J.E. Page, A. Dipple, Mutational spectra for polycyclic aromatic hydrocarbons in the supF target gene, Mutat. Res. 450 (2000) 75–93.
[7] L. Yang, V.M. Maher, J.J. McCormick, Kinds of mutations formed when a shuttle vector containing adducts of (±)-7beta, 8alpha-dihydroxy-9alpha, 10alpha-epoxy-7,8,9,10-tetrahydrobenzo[*a*]pyrene replicates in human cells, Proc. Natl. Acad. Sci. USA 84 (1987) 3787–3791.
[8] M.A. Wani, Q. Zhu, M. El-Mahdy, S. Venkatachalam, A.A. Wani, Enhanced sensitivity to anti-benzo(*a*)pyrene-diol-epoxide DNA damage correlates with decreased global genomic repair attributable to abrogated p53 function in human cells, Cancer Res. 60 (2000) 2273–2280.
[9] S. Mukhopadhyay, D.R. Clark, N.B. Watson, W. Zacharias, W.G. McGregor, REV1 accumulates in DNA damage-induced nuclear foci in human cells and is implicated in mutagenesis by benzo[*a*]pyrenediolepoxide, Nucleic Acids Res. 32 (2004) 5820–5826.
[10] A. Stanisławska-Sachadyn, P. Sachadyn, K. Ihle, C. Sydorczuk, K. Wiejacha, J. Kur, The construction of bifunctional fusion proteins consisting of MutS and GFP, J. Biotechnol. 121 (2006) 134–143.
[11] R. Heim, A.B. Cubitt, R.Y. Tsien, Improved green fluorescence, Nature 373 (1995) 663–664.
[12] R. Heim, R.Y. Tsien, Engineering green fluorescent protein for improved brightness, longer wavelengths and fluorescence resonance energy transfer, Curr. Biol. 6 (1996) 178–182.
[13] N.F. Cariello, S. Narayanan, P. Kwanyuen, H. Muth, W.M. Casey, A novel bacterial reversion and forward mutation assay based on green fluorescent protein, Mutat. Res. 414 (1998) 95–105.
[14] M. Yu, T. Chalfie, G. Guskirchen, W.W. Ward, D.C. Parsher, Green fluorescent protein as a marker for gene expression, Science 263 (1994) 802–805.
[15] S.W. Kohler, G.S. Provost, A. Fieck, P.L. Kretz, W.O. Bullock, J.A. Sorge, D.D. Levy, J.D. Groopman, S.E. Lim, M.M. Seidman, K.H. Kraemer, Spectra of spontaneous and mutagen-induced mutations in the lacI gene in transgenic mice, Cancer Res. 52 (1992) 5668–5673.
[16] M.F. Denissenko, J. Cahill, T.B. Koudriakova, N. Gerber, G.P. Pfeifer, Quantitation and mapping of aflatoxin B1-induced DNA damage in genomic DNA using aflatoxin B1-8,9-epoxide and microsomal activation systems, Mutat. Res. 425 (1999) 205–211.
[17] N.E. Geacintov, D. Zinger, V. Ibanez, R. Santella, D. Grunberger, R.G. Harvey, Properties of covalent benzo[*a*]pyrene diol epoxide–DNA adducts investigated by fluorescence techniques, Carcinogenesis 8 (1987) 925–935.
[18] P. Chary, R.S. Lloyd, *In vitro* replication by prokaryotic and eukaryotic polymerases on DNA templates containing site-specific and stereospecific benzo[*a*]pyrene-7, 8-dihydrodiol-9, 10-epoxide adducts, Nucleic Acids Res. 23 (1995) 1398–1405.
[19] N. Billinton, M.G. Barker, C.E. Michel, A.W. Knight, W.-D. Heyer, N.J. Goddard, P.R. Fielden, R.M. Walmsley, Development of a green fluorescent protein reporter for a yeast genotoxicity biosensor, Biosens. Bioelectron. 13 (1998) 831–838.
[20] Y.H. Hsiang, R. Hertzberg, S. Hecht, L.F. Liu, Camptothecin induced protein-linked DNA breaks via mammalian DNA topoisomerase I, J. Biol. Chem. 260 (1985) 14873–14878.
[21] C. Jaxel, K.W. Kohn, P. Yves, Topoisomerase I interaction with SV4O DNA in the presence and absence of camptothecin, Nucleic Acids Res. 16 (1988) 11157–11170.
[22] S.E. Porter, J.J. Champoux, The basis for camptothecin enhancement of DNA breakage by eukaryotic topoisomerase I, Nucleic Acids Res. 17 (1989) 8521–8532.
[23] K. Tanizawa, K.W. Kohn, G. Kohlhagen, F. Leteurtre, Y. Pommier, Differential stabilization of eukaryotic DNA topoisomerase I cleavable complexes by camptothecin derivatives, Biochemistry 34 (1995) 7200–7206.
[24] Y. Pommier, G. Kohlhagen, P. Pourquier, J.M. Sayer, H. Kroth, D.M. Jerina, Benzo[*a*]pyrene diol epoxide adducts in DNA are potent suppressors of a normal topoisomerase I cleavage site and powerful inducers of other topoisomerase I cleavages, Proc. Natl. Acad. Sci. USA 97 (2000) 2040–2045.
[25] M. Lodovici, C. Luceri, F. Guglielmi, C. Bacci, V. Akpan, M.L. Fonnesu, V. Boddi, P. Dolara, Benzo(*a*)pyrene diolepoxide (BPDE)–DNA adduct levels in leukocytes of smokers in relation to polymorphism of CYP1A1,GSTM1,GSTP1,GSTT1, and mEH, Cancer Epidemiol. Biomarkers Prev. 13 (2004) 1342–1348.
[26] H. Bartsch, U. Nair, A. Risch, M. Rojas, H. Wilkman, K. Alexandrov, Genetic polymorphism of CYP genes, alone or in combination, as a risk modifier of tobacco-related cancers, Cancer Epidemiol. Biomarkers Prev. 9 (2000) 3–28.
[27] D. Ryberg, V. Skaug, A. Hewer, H. David, P. Lorna, W. Harries, C. Roland, C.R. Wolf, D. Øgreid, A. Ulvik, P. Vu, A. Haugen, Genotypes of glutathione transferase M1 and P1 and their significance for lung DNA adduct levels and cancer risk, Carcinogenesis 18 (1997) 1285–1289.